

# Propagation behaviors of guided waves in graphene platelet reinforced metal foam plates

Wubin Shan<sup>1,2</sup>, Hao Zhong<sup>1</sup>, Nannan Zhang<sup>1</sup> and Guilin She<sup>\*3</sup>

<sup>1</sup>Hunan Electrical College of Technology, School of elevator engineering, Xiangtan 411100, China

<sup>2</sup>College of Mechanical and Vehicle Engineering, Hunan University, Changsha 410082, China

<sup>3</sup>College of Mechanical and Vehicle Engineering, Chongqing University, Chongqing 400044, China

(Received July 21, 2023, Revised August 28, 2023, Accepted November 27, 2023)

**Abstract.** At present, the research on wave propagation in graphene platelet reinforced composite plates focuses on the propagation behavior of bulk waves, in which the effect of boundary condition is ignored, there is no literature report on propagation behaviors of guided waves in graphene platelet reinforced metal foams (GPLRMF) plates. In fact, wave propagation is affected by boundary conditions, so it is necessary to study the propagation characteristics of guided waves. The aim of this paper is to solve this problem. The effective performance of the material was calculated using the mixing law. Equations of motion of GPLRMF plate is derived by using Hamilton's principle. Then, the eigenvalue method is used to obtain the expressions of bending wave, shear wave and longitudinal wave, and the degradation verification is carried out. Finally, the effects of graphene platelets (GPLs) volume fraction, elastic foundation, porosity coefficient, GPLs distribution types and porosity distribution types on the dispersion relations are studied. We find that these factors play an important role in the propagation characteristics and phase velocity of guided waves.

**Keywords:** galerkin principle; graphene platelets; metal foams; phase velocity; platephase velocity; wave propagation

## 1. Introduction

At present, studying the static and dynamic behavior of functionally graded or reinforced structures has become a hot research topic, such as literatures (Ahmadi *et al.* 2021, Allahkarami and Tohidi 2022, Aris and Ahmadi 2022, Assie *et al.* 2023, Hendi *et al.* 2022, Malikan *et al.* 2022, Mahani *et al.* 2020, Martins *et al.* 2021, Melaibari *et al.* 2023, Nguyen *et al.* 2021, Phuong *et al.* 2022, 2021, Ramezani *et al.* 2022, Saiah *et al.* 2022, Shahgholian-Ghahfarokhi *et al.* 2021, Salehi *et al.* 2022, Trang *et al.* 2022, Van Doan *et al.* 2022, Alnujaie *et al.* 2021, Gan and She 2023, She 2021, She and Li 2022, Xu and She 2022, Zhang *et al.* 2023c, 2023d, Ahmadi and Foroutan 2021, Abuteir and Boutagouga 2022, Basha *et al.* 2022, Wang and Zhang 2022, Alazwari *et al.* 2022, Daikh *et al.* 2021, 2023, Mohamed *et al.* 2023, Chen *et al.* 2022a, b, Ding *et al.* 2021, 2023a, b, Ding *et al.* 2023a, b, c, 2022a, b, Gan and She 2023, Gan *et al.* 2023, Li *et al.* 2023, She 2021, She and Ding 2023, She and Li 2022, She *et al.* 2021, 2022, Wu and She 2023, Xu and She 2022, 2023, Xu *et al.* 2023a, b, c, 2024, Zhang and She 2022, 2023a, b, 2024, Zhang *et al.* 2021, 2022, 2023a, b, c, d, e, Zhao *et al.* 2022a, b, Ding and She 2023c, Ding *et al.* 2023d, Gan and She 2024, Shan and She 2023), but there are relatively few literatures on wave propagation problems.

For example, Xiang *et al.* (2023) analyzed the wave

propagation phenomenon of graphene oxide powder-strengthened composite curved beam. Gan *et al.* (2023) discussed the wave propagation of GPLRMF circular plates using Laplace integral method. Ebrahimi and Seyfi (2022) studied wave propagation behaviors of GPLRMF plates rested on an elastic medium subjected to hygro-thermal effects. Hashemi-Nejad *et al.* (2022) examined wave propagation in GPLRMF composite rotating thin-walled blades with nonuniform and uniform distributions of graphene platelet. Babaei *et al.* (2021) performed the stress wave propagation analysis of GPLRMF joined conical-cylindrical-conical shell using the modified Halpin-Tsai estimation. Al Mukahal *et al.* (2021) presented wave propagation of GPLRMF curved beams having auxetic core with viscoelastic foundation with the aid of the differential quadrature method. Zenkour and Sobhy (2022) investigated the axial magnetic effect on wave propagations in graphene platelet-reinforced beams in nano scale. Li and Han (2021) analyzed the guided waves propagation of graphene-epoxy core and piezoelectric shells using the Chebyshev spectral element method. Li *et al.* (2020) presented wave propagation analysis in piezoelectric graphene platelets plates with the semi-analytical method. Li and Han (2021) discussed wave propagation in graphene reinforced composite annular plates via semi-analytical method. Ebrahimi and Dabbagh (2020) developed a nonlocal strain gradient theory to analyze wave dispersions of axially loaded graphene sheets resting on the viscoelastic foundations. Ebrahimi *et al.* (2021) analyzed wave propagation of spinning GPLRMF cylindrical shell at nano scale.

\*Corresponding author, Associate Professor  
E-mail: sheguilin@cqu.edu.cn

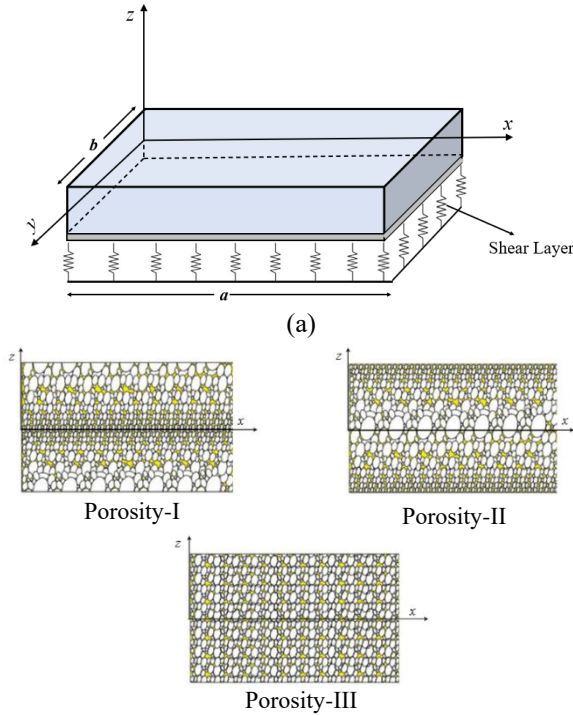


Fig. 1 A sketch of GPLRMF plate resting on elastic foundation (Modified from Zhang *et al.* 2023b, Ding and She 2023a)

At present, there is no literature report on propagation behaviors of guided waves in graphene platelet plate reinforced metal foam (GPLRMF) plates. Through literature search, we can see that there is very little papers about the propagation of guided waves, and currently, there are no literature reporting on the guided wave in the GPLRMF plates. In fact, wave propagation is affected by boundary conditions, the aim of this paper is to solve this problem.

## 2. Wave equations

Illustrated in Fig. 1 is the schematic diagram of a GPLRMF plate, in addition the plate rests on two-parameters elastic foundation  $p(x, y) = k_w w - k_s \left( \frac{\partial^2 w}{\partial x^2} + \frac{\partial^2 w}{\partial y^2} \right)$ .

The material characteristics may be expressed as (Kitipornchai *et al.* 2017)

$$\begin{aligned}
 E(z, T) &= \begin{cases} E^\# [1 - e_1 \cos(\pi z / h)], & \text{(Porosity-I)} \\ E^\# \{1 - e_2 [1 - \cos(\pi z / h)]\}, & \text{(Porosity-II)} \\ E^\# e_3, & \text{(Porosity-III)} \end{cases} \\
 \rho(z, T) &= \begin{cases} \rho^\# [1 - e_{m1} \cos(\pi z / h)], & \text{(Porosity-I)} \\ \rho^\# \{1 - e_{m2} [1 - \cos(\pi z / h)]\}, & \text{(Porosity-II)} \\ \rho^\# e_{m3}, & \text{(Porosity-III)} \end{cases} \\
 \alpha(z) &= \alpha^\# \\
 \mu(z) &= \mu^\#
 \end{aligned} \quad (1)$$

In which (Kitipornchai *et al.* 2017)

$$\begin{aligned}
 E^\# &= \frac{3}{8} \left( \frac{1 + \zeta_L V_{GPL} \eta_L}{1 - \eta_L V_{GPL}} \right) \times E_M + \frac{5}{8} \left( \frac{1 + \zeta_W V_{GPL} \eta_W}{1 - \eta_W V_{GPL}} \right) \times E_M \\
 \begin{bmatrix} \rho^\# \\ \alpha^\# \\ \mu^\# \end{bmatrix} &= V_{GPL} \begin{bmatrix} \rho_{GPL} \\ \alpha_{GPL} \\ \mu_{GPL} \end{bmatrix} + (1 - V_{GPL}) \begin{bmatrix} \rho_M \\ \alpha_M \\ \mu_M \end{bmatrix}
 \end{aligned} \quad (2)$$

In addition (Kitipornchai *et al.* 2017)

$$\frac{E(z, T)}{E_c} = \left[ \frac{\rho(z)}{\rho_c} \right]^2 \quad (3)$$

$$\begin{cases} 1 - e_{m1} \cos(\pi z / h) = \sqrt{1 - e_1 \cos(\pi z / h)} \\ 1 - e_{m2} [1 - \cos(\pi z / h)] = \sqrt{1 - e_2 [1 - \cos(\pi z / h)]} \\ e_{m3} = \sqrt{e_3} \end{cases} \quad (4)$$

Due to the fact (Zhang *et al.* 2023b, Ding and She 2023a)

$$\begin{aligned}
 \int_0^{\frac{h}{2}} \sqrt{1 - e_1 \cos(\pi z / h)} dz &= \int_0^{\frac{h}{2}} \sqrt{e_3} dz \\
 &= \int_0^{\frac{h}{2}} \sqrt{1 - e_2 [1 - \cos(\pi z / h)]} dz
 \end{aligned} \quad (5)$$

Considering that (Zhang *et al.* 2023b, Ding and She 2023a)

$$V_{GPL} = \begin{cases} Si_1 [1 - \cos(\pi z / h)], & \text{(GPL-A)} \\ Si_2 \cos(\pi z / h), & \text{(GPL-B)} \\ Si_3, & \text{(GPL-C)} \end{cases} \quad (6)$$

Herein, the value of coefficients  $Si_1$ ,  $Si_2$ , and  $Si_3$  refers to Ref. (Kitipornchai *et al.* 2017).

The adopted displacement field is (Sun and Luo 2012)

$$\begin{aligned}
 u &= u_0(x, y, t) + z\varphi_x(x, y, t) \\
 v &= v_0(x, y, t) + z\varphi_y(x, y, t) \\
 w &= w_0(x, y, t)
 \end{aligned} \quad (7)$$

here,  $u_0$ ,  $v_0$ ,  $w_0$  are the plate displacements,  $\varphi_x$  and  $\varphi_y$  are the mid-plane rotation. The strains are (Sun and Luo 2012)

$$\begin{aligned}
 \varepsilon_x &= z \frac{\partial \varphi_x}{\partial x} + \frac{\partial u_0}{\partial x}, \quad \varepsilon_y = z \frac{\partial \varphi_y}{\partial y} + \frac{\partial v_0}{\partial y}, \\
 \varepsilon_{xy} &= z \left( \frac{\partial \varphi_x}{\partial y} + \frac{\partial \varphi_y}{\partial x} \right) + \frac{\partial u_0}{\partial y} + \frac{\partial v_0}{\partial x}, \\
 \varepsilon_{xz} &= \frac{\partial w_0}{\partial x} + \varphi_x, \quad \varepsilon_{yz} = \frac{\partial w_0}{\partial y} + \varphi_y.
 \end{aligned} \quad (8)$$

The stress-strain relationship is,

$$\begin{Bmatrix} \sigma_x \\ \sigma_y \\ \sigma_{xy} \\ \sigma_{xz} \\ \sigma_{yz} \end{Bmatrix} = \begin{bmatrix} \frac{E(z)}{1-\nu^2} & G(z) & 0 & 0 & 0 \\ G(z) & \frac{E(z)}{1-\nu^2} & 0 & 0 & 0 \\ 0 & 0 & G(z) & 0 & 0 \\ 0 & 0 & 0 & \frac{5}{6}G(z) & 0 \\ 0 & 0 & 0 & 0 & \frac{5}{6}G(z) \end{bmatrix} \begin{Bmatrix} \frac{\partial u_0}{\partial x} + z \frac{\partial \varphi_x}{\partial x} \\ \frac{\partial v_0}{\partial y} + z \frac{\partial \varphi_y}{\partial y} \\ \frac{\partial u_0}{\partial y} + \frac{\partial v_0}{\partial x} + z \left( \frac{\partial \varphi_x}{\partial y} + \frac{\partial \varphi_y}{\partial x} \right) \\ \varphi_x + \frac{\partial w_0}{\partial x} \\ \varphi_y + \frac{\partial w_0}{\partial y} \end{Bmatrix} \quad (9)$$

The stress resultants and couples have the following form,

$$\begin{aligned} N_x &= A_{11} \frac{\partial u_0}{\partial x} + A_{12} \frac{\partial v_0}{\partial y}, N_y = A_{12} \frac{\partial u_0}{\partial x} + A_{22} \frac{\partial v_0}{\partial y}, \\ N_{xy} &= A_{66} \left( \frac{\partial u_0}{\partial y} + \frac{\partial v_0}{\partial x} \right), M_x = D_{11} \frac{\partial \varphi_x}{\partial x} + D_{12} \frac{\partial \varphi_y}{\partial y}, \\ M_y &= D_{12} \frac{\partial \varphi_x}{\partial x} + D_{22} \frac{\partial \varphi_y}{\partial y}, Q_x = A_{44} \left( \varphi_x + \frac{\partial w_0}{\partial x} \right), \\ Q_y &= A_{55} \left( \varphi_y + \frac{\partial w_0}{\partial y} \right). \end{aligned} \quad (10)$$

in which (Sun and Luo 2012)

$$\begin{aligned} A_{11} &= A_{22} = \int_{-\frac{h}{2}}^{\frac{h}{2}} \frac{E(z)}{1-\nu^2} dz, A_{12} = \int_{-\frac{h}{2}}^{\frac{h}{2}} \frac{\nu E(z)}{1-\nu^2} dz, A_{66} = \int_{-\frac{h}{2}}^{\frac{h}{2}} G(z) dz, \\ A_{44} &= A_{55} = \gamma^2 A_{66}, D_{11} = D_{22} = \int_{-\frac{h}{2}}^{\frac{h}{2}} \frac{z^2 E(z)}{1-\nu^2} dz, \\ D_{12} &= \int_{-\frac{h}{2}}^{\frac{h}{2}} \frac{z^2 \nu E(z)}{1-\nu^2} dz, D_{66} = \int_{-\frac{h}{2}}^{\frac{h}{2}} z^2 G(z) dz. \end{aligned} \quad (11)$$

Using the Euler-Lagrange principle, the motion equations can be obtained as (Sun and Luo 2012)

$$\begin{aligned} \frac{\partial N_x}{\partial x} + \frac{\partial N_{xy}}{\partial y} &= I_0 \frac{\partial^2 u_0}{\partial t^2}, \\ \frac{\partial N_y}{\partial y} + \frac{\partial N_{xy}}{\partial x} &= I_0 \frac{\partial^2 v_0}{\partial t^2}, \\ \frac{\partial Q_x}{\partial x} + \frac{\partial Q_y}{\partial y} + \frac{\partial}{\partial x} \left( N_x \frac{\partial w}{\partial x} + k_s \frac{\partial w}{\partial x} + N_{xy} \frac{\partial w}{\partial y} \right) \\ + \frac{\partial}{\partial y} \left( N_y \frac{\partial w}{\partial y} + k_s \frac{\partial w}{\partial y} + N_{xy} \frac{\partial w}{\partial x} \right) + k_w w &= I_0 \frac{\partial^2 w_0}{\partial t^2}, \\ \frac{\partial M_x}{\partial x} + \frac{\partial M_{xy}}{\partial y} - Q_x &= I_2 \frac{\partial^2 \varphi_x}{\partial t^2}, \\ \frac{\partial M_y}{\partial y} + \frac{\partial M_{xy}}{\partial x} - Q_y &= I_2 \frac{\partial^2 \varphi_y}{\partial t^2}. \end{aligned} \quad (12)$$

Herein,  $(I_0, I_2) = \int_{-\frac{h}{2}}^{\frac{h}{2}} \rho(z)(1, z^2) dz$ .

Using Eq. (10), Eq. (12) becomes

$$\begin{aligned} A_{11} \frac{\partial^2 u_0}{\partial x^2} + A_{12} \frac{\partial^2 v_0}{\partial x \partial y} + A_{66} \left( \frac{\partial^2 u_0}{\partial y^2} + \frac{\partial^2 v_0}{\partial x \partial y} \right) &= I_0 \frac{\partial^2 u_0}{\partial t^2}, \\ A_{12} \frac{\partial^2 u_0}{\partial x \partial y} + A_{22} \frac{\partial^2 v_0}{\partial y^2} + A_{66} \left( \frac{\partial^2 u_0}{\partial x \partial y} + \frac{\partial^2 v_0}{\partial x^2} \right) &= I_0 \frac{\partial^2 v_0}{\partial t^2}, \\ A_{44} \left( \frac{\partial \varphi_x}{\partial x} + \frac{\partial^2 w_0}{\partial x^2} \right) + A_{55} \left( \frac{\partial \varphi_y}{\partial y} + \frac{\partial^2 w_0}{\partial y^2} \right) + K_s \left( \frac{\partial^2 w_0}{\partial x^2} + \frac{\partial^2 w_0}{\partial y^2} \right) \\ + k_w w &= I_0 \frac{\partial^2 w_0}{\partial t^2}, \\ D_{11} \frac{\partial^2 \varphi_x}{\partial x^2} + D_{12} \frac{\partial^2 \varphi_y}{\partial x \partial y} + D_{66} \left( \frac{\partial^2 \varphi_x}{\partial y^2} + \frac{\partial^2 \varphi_y}{\partial x \partial y} \right) - A_{44} \left( \varphi_x + \frac{\partial w_0}{\partial x} \right) &= I_2 \frac{\partial^2 \varphi_x}{\partial t^2}, \\ D_{12} \frac{\partial^2 \varphi_x}{\partial x \partial y} + D_{22} \frac{\partial^2 \varphi_y}{\partial y^2} + D_{66} \left( \frac{\partial^2 \varphi_x}{\partial x \partial y} + \frac{\partial^2 \varphi_y}{\partial x^2} \right) - A_{55} \left( \varphi_y + \frac{\partial w_0}{\partial y} \right) &= I_2 \frac{\partial^2 \varphi_y}{\partial t^2}. \end{aligned} \quad (13)$$

### 3. Solution method

Considering clamped supported ends, the following solutions may be adopted (Sun and Luo 2012)

$$\begin{aligned} u_0(x, y, t) &= \sum_{m,n=1,3,5,\dots} u_{mn}(t) \sin\left(\frac{m\pi}{a}x\right) \sin\left(\frac{n\pi}{b}y\right) \\ &\times \left[ e^{i(\kappa_1 x + \kappa_2 y + \omega t)} + e^{i(\kappa_1 x + \kappa_2 y - \omega t)} \right], \\ v_0(x, y, t) &= \sum_{m,n=1,3,5,\dots} v_{mn}(t) \sin\left(\frac{m\pi}{a}x\right) \sin\left(\frac{n\pi}{b}y\right) \\ &\times \left[ e^{i(\kappa_1 x + \kappa_2 y + \omega t)} + e^{i(\kappa_1 x + \kappa_2 y - \omega t)} \right], \\ w_0(x, y, t) &= \sum_{m,n=1,3,5,\dots} w_{mn}(t) [1 - \cos\left(\frac{2m\pi}{a}x\right)] [1 - \cos\left(\frac{2n\pi}{b}y\right)] \\ &\times \left[ e^{i(\kappa_1 x + \kappa_2 y + \omega t)} + e^{i(\kappa_1 x + \kappa_2 y - \omega t)} \right], \\ \varphi_x(x, y, t) &= \sum_{m,n=1,3,5,\dots} \varphi_{mn}^x(t) \sin\left(\frac{2m\pi}{a}x\right) [1 - \cos\left(\frac{2n\pi}{b}y\right)] \\ &\times \left[ e^{i(\kappa_1 x + \kappa_2 y + \omega t)} + e^{i(\kappa_1 x + \kappa_2 y - \omega t)} \right], \\ \varphi_y(x, y, t) &= \sum_{m,n=1,3,5,\dots} \varphi_{mn}^y(t) [1 - \cos\left(\frac{2m\pi}{a}x\right)] \sin\left(\frac{2n\pi}{b}y\right) \\ &\times \left[ e^{i(\kappa_1 x + \kappa_2 y + \omega t)} + e^{i(\kappa_1 x + \kappa_2 y - \omega t)} \right]. \end{aligned} \quad (14)$$

In which,  $[u_{mn}, v_{mn}, w_{mn}, \varphi_{mn}^x, \varphi_{mn}^y]$  are wave amplitudes,  $[\kappa_1, \kappa_2]$  are wave numbers. Using Eq. (14) and Galerkin principle, Eq. (13) becomes (She 2021)

$$\begin{pmatrix} K_{11} & K_{12} & K_{13} & K_{14} & K_{15} \\ K_{21} & K_{22} & K_{23} & K_{24} & K_{25} \\ K_{31} & K_{32} & K_{33} & K_{34} & K_{35} \\ K_{41} & K_{42} & K_{43} & K_{44} & K_{45} \\ K_{51} & K_{52} & K_{53} & K_{54} & K_{55} \end{pmatrix} - \omega^2 \begin{pmatrix} I_0 & 0 & 0 & 0 & 0 \\ 0 & I_0 & 0 & 0 & 0 \\ 0 & 0 & 9I_0 & 0 & 0 \\ 0 & 0 & 0 & 3I_2 & 0 \\ 0 & 0 & 0 & 0 & 3I_2 \end{pmatrix} \begin{pmatrix} u_{mn} \\ v_{mn} \\ w_{mn} \\ \varphi_{mn}^x \\ \varphi_{mn}^y \end{pmatrix} = 0 \quad (15)$$

$$[u_{11}, v_{11}, w_{11}, \varphi_{11}^x, \varphi_{11}^y]^T = 0$$

In which

$$\begin{aligned} K_{11} &= A_{11} (\lambda_1^2 + \kappa_1^2) + A_{66} (\mu_1^2 + \kappa_2^2), \\ K_{12} &= K_{21} = (A_{12} + A_{66}) \kappa_1 \kappa_2, \\ K_{13} &= K_{31} = K_{14} = K_{41} = K_{15} = K_{51} = K_{23} \\ &= K_{32} = K_{24} = K_{42} = K_{25} = K_{52} = 0, \\ K_{22} &= A_{22} (\mu_1^2 + \kappa_2^2) + A_{66} (\lambda_1^2 + \kappa_1^2), \\ K_{33} &= 9[(A_{44} + K_s) \kappa_1^2 + (A_{55} + K_s) \kappa_2^2] \\ &+ 12[(A_{44} + K_s) \lambda_1^2 + (A_{55} + K_s) \mu_1^2] + K_w, \\ K_{34} &= K_{43} = 6A_{44} \lambda_1, K_{35} = K_{53} = 6A_{55} \mu_1, \\ K_{44} &= 3D_{11} (4\lambda_1^2 + \kappa_1^2) + D_{66} (4\mu_1^2 + \kappa_2^2) + 3A_{44}, \\ K_{45} &= K_{54} = 4(D_{12} + D_{66}) \lambda_1 \mu_1, \\ K_{55} &= 3D_{22} (4\mu_1^2 + \kappa_2^2) + D_{66} (4\lambda_1^2 + \kappa_1^2) + 3A_{55}. \end{aligned}$$

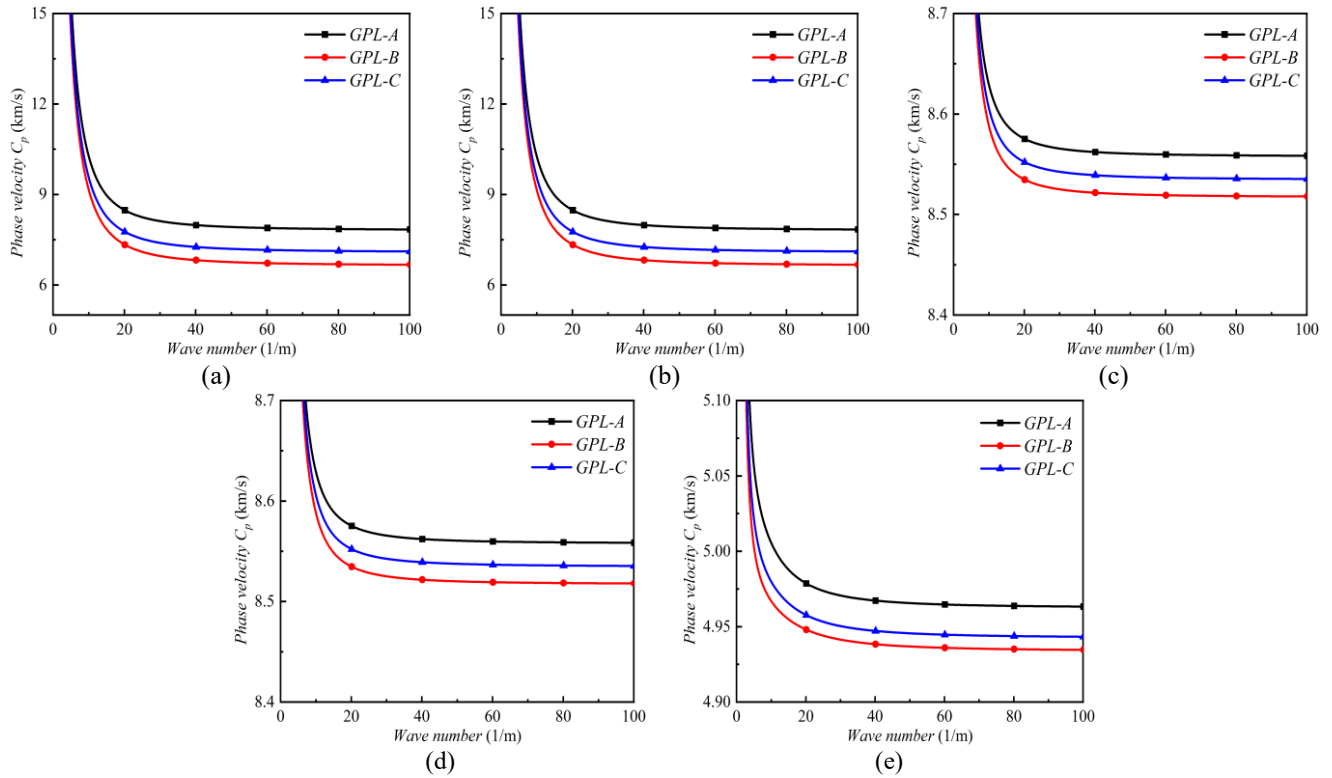


Fig. 2 Effect of GPLs distribution types ( $a=b=2$  m,  $h=0.2$  m,  $k_w=0$ ,  $k_s=0$ , Porosity-I,  $W_{gp}=1\%$ ,  $e_1=0.2$ )

in which,  $\lambda_1 = \frac{\pi}{a}$ ,  $\mu_1 = \frac{\pi}{b}$ . If Eq. (15) has a non-zero solution, then the determinant of the matrix of Eq. (15) must be equal to 0, from which five different solutions can be obtained. The largest two solutions correspond to shear waves, the smallest solution corresponds to bending waves, and the other two solutions correspond to longitudinal waves. We can get the expressions of phase velocity  $C_p = \frac{\omega}{\kappa}$  from Eq. (15) with the consideration of  $\kappa = \kappa_1 = \kappa_2$ .

#### 4. Numerical analyses

In the next part, the adopted geometrical parameters and material properties are (Gan *et al.* 2023, Gan and She 2023):  $E_m=200$  GPa,  $\mu_m=0.33$ ,  $\rho_m=7850$  kg/m<sup>3</sup>,  $E_{GPL}=1010$  GPa,  $\mu_{GPL}=0.186$ ,  $\rho_{GPL}=1060$  kg/m<sup>3</sup>,  $t_{GPL}=1.5 \times 10^{-9}$  m,  $w_{GPL}=2.5 \times 10^{-6}$  m,  $l_{GPL}=1.5 \times 10^{-6}$  m.

In the following analysis, in Figs. 2 to 6, the first and second figures are shear waves, the third and fourth figures are longitudinal waves, and the fifth figure is bending waves.

In Fig. 2, we studied the impact of three GPLs distribution types, GPL-A, GPL-B and GPL-C, on wave propagation. As seen, when the wave number is small, the phase velocity decreases sharply with the increase of the wave number. This indicates that only when the wave number is very small, the wave number have a significant impact on the phase velocity. When the wave number increases to a certain value, the phase velocity tends to be

stable, and at this time, the value of the bending wave is the smallest. This is because, similar to vibration problems, bending waves are the most important issue which should be considered in wave propagation problems. Additionally, the values of phase velocity can be ranked in order as follows: GPL-A>GPL-C>GPL-B. This is because for the GPL-A type, the content of GPLs is highest on the upper and lower surfaces of the plate, while for the GPL-B type, the content of GPLs is lowest on the upper and lower surfaces of the plate. In addition, when the wave number is fixed, the phase velocity of shear wave is greater than the phase velocity of longitudinal wave and the phase velocity of bending wave.

In Fig. 3, we studied the impact of three porosity distribution types on wave propagation problems. It can be seen that when the wave number is small, the phase velocity decreases sharply with the increase of wave number. When the wave number increases to a certain value, the phase velocity tends to be stable, and at this time, the value of bending wave is the smallest; When the wave number keeps unchanged, the values of phase velocity can be ranked in order as follows: Porosity-I>Porosity-III>Porosity-II. This is because for the Porosity-I type, the porosity is highest on the upper and lower surfaces of the plate, while for the Porosity-II type, the porosity is lowest on the upper and lower surfaces of the plate.

In Fig. 4, we studied the effect of porosity coefficient. As seen, under a certain wave number, the phase velocity is the minus function of the porosity coefficient, that is, the larger the porosity coefficient, the smaller the phase velocity. As expected, the higher the porosity coefficient, the lower the stiffness of the plate, resulting in a decrease in

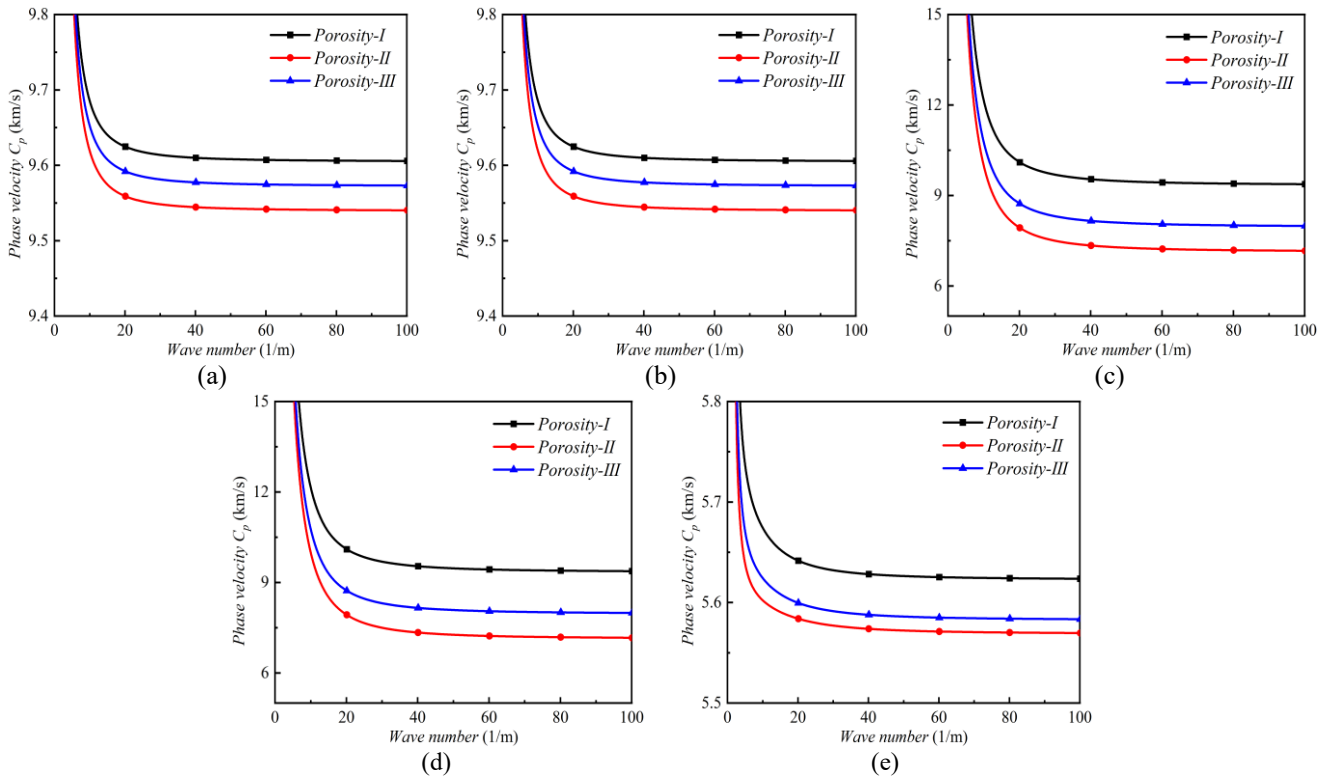


Fig. 3 Effect of porosity distribution types ( $a=b=2$  m,  $h=0.2$  m,  $k_w=0$ ,  $k_s=0$ , GPL-A,  $W_{gpl}=1\%$ ,  $e_1=0.2$ )

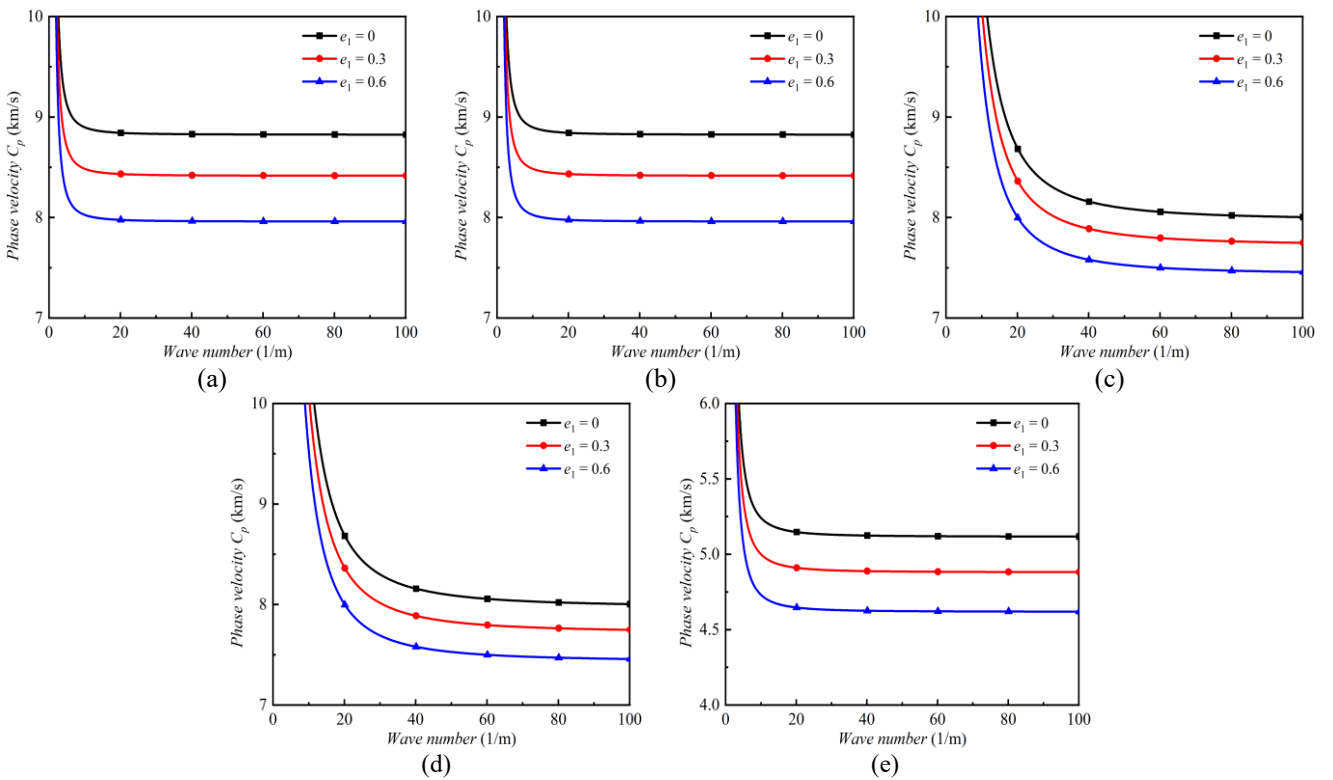


Fig. 4 Effect of porosity coefficient ( $a=b=2$  m,  $h=0.2$  m,  $k_w=0$ ,  $k_s=0$ , Porosity-I,  $W_{gpl}=1\%$ , GPL-A)

phase velocity. In addition, at the same wave number, the phase velocity of shear wave is the largest, followed by longitudinal wave, and bending wave.

In Fig. 5, we studied the impact of GPLs weight fraction on wave propagation problems. As seen, the GPLs weight fraction play an important role in wave propagation. Under

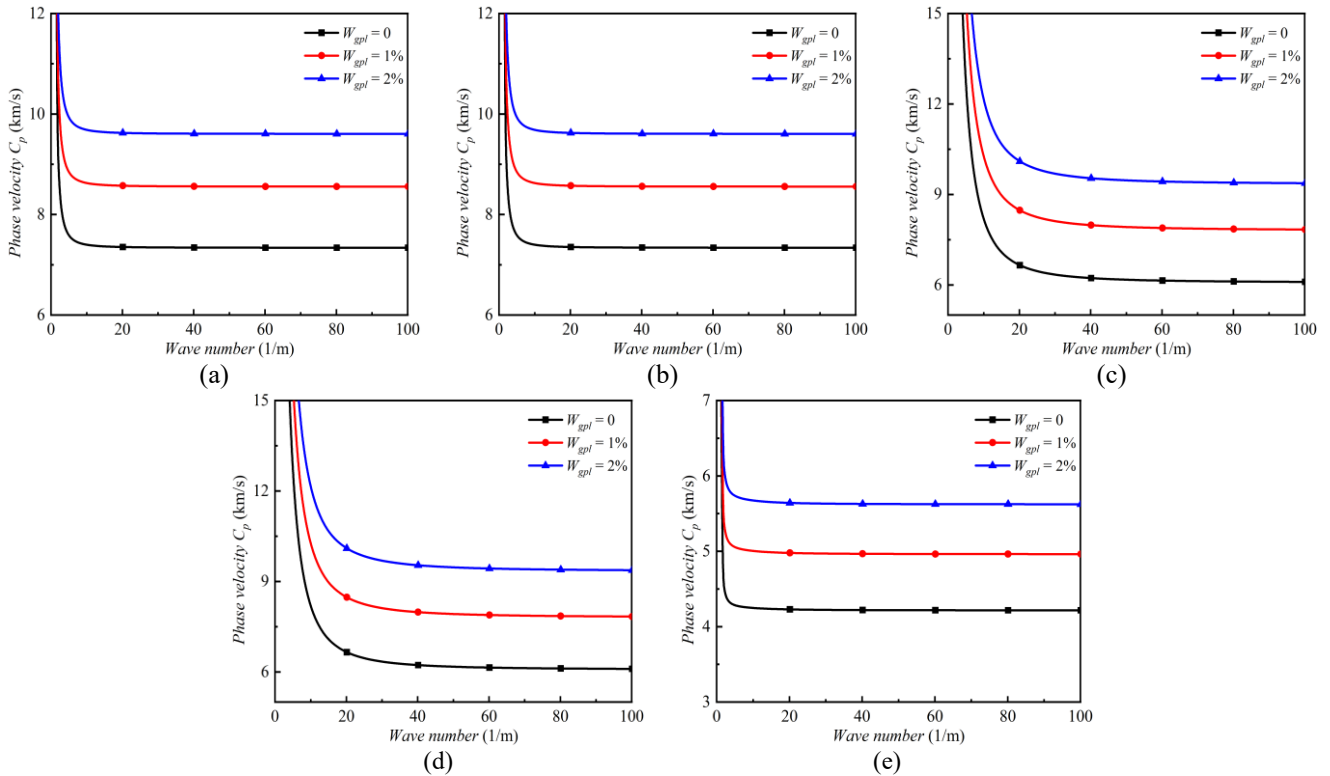


Fig. 5 Effect of porosity coefficient ( $a=b=2$  m,  $h=0.2$  m,  $k_w=0$ ,  $k_s=0$ , Porosity-I, GPL-A,  $e_1=0.2$ )

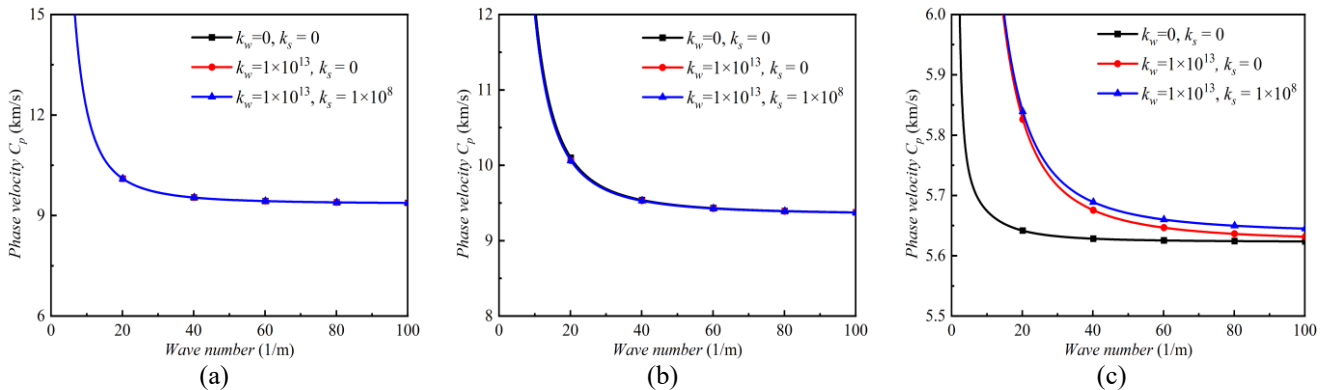


Fig. 6 Effect of porosity coefficient ( $a=b=2$  m,  $h=0.2$  m, GPL-A, Porosity-I,  $W_{GPL}=1\%$ ,  $e_1=0.2$ )

a certain wave number, the phase velocity increases significantly with the increase of GPLs weight fraction. As expected, the higher the GPLs weight fraction, the higher the stiffness of the plate, resulting in an increase in phase velocity. In addition, the larger the wave number, the smaller the phase velocity. In addition, at the same wave number, the phase velocity of shear wave is the largest, followed by longitudinal wave and bending wave.

In Fig. 6, we studied the impact of elastic foundation on wave propagation. It can be seen that the impact of elastic foundation on shear wave is negligible, but the impact of elastic foundation on bending wave is more significant. When  $k$  is large, the larger the  $k_w$  or  $k_s$ , the greater the phase velocity. This is because, similar to vibration problems, elastic foundations only have a significant impact on bending vibration problems or the propagation of bending waves.

### 5. Conclusions

As an innovative attempt, the propagation of longitudinal, bending and shear waves in GPLRMF plates resting on elastic foundations are studied in this paper. The material properties of GPLs and porosity change smoothly along the thickness of the plate. Subsequently, the governing equations are solved based on Galerkin principle and the conclusions are given as,

- (1) When the wave number is small, the phase velocity decreases sharply with the increase of the wave number. The values of phase velocity can be ranked in order as follows: GPL-A>GPL-C>GPL-B.
- (2) When the wave number keeps unchanged, the phase velocity of shear wave is greater than longitudinal wave and bending wave.

- (3) When the wave number keeps unchanged, the values of phase velocity can be ranked in order as follows: Porosity-I>Porosity-III>Porosity-II.
- (4) Under a certain wave number, phase velocity decreases significantly with the increase of porosity coefficient.
- (5) Under a certain wave number, the phase velocity increases significantly as the GPLs weight fraction rises.
- (6) The impact of elastic foundation on shear wave can be ignored, but the influence of elastic foundation on bending wave is more significant. The larger the  $k_w$  or  $k_s$ , the larger the phase velocity.

## Acknowledgments

The present work is supported by "Natural Science Foundation of Hunan Province" (2022JJ60022).

## References

- Abuteir, B.W. and Boutagouga, D. (2022), "Free-vibration response of functionally graded porous shell structures in thermal environments with temperature-dependent material properties", *Acta Mech.*, **233**(11), 4877-4901. <https://doi.org/10.1007/s00707-022-03351-y>.
- Ahmadi, H. and Foroutan, K. (2021), "Nonlinear buckling analysis of FGP shallow spherical shells under thermomechanical condition," *Steel. Compos. Struct.*, **40**(4), 555-570. <https://doi.org/10.12989/scs.2021.40.4.555>.
- Ahmadi, H., Bayat, A. and Duc, N.D. (2021), "Nonlinear forced vibrations analysis of imperfect stiffened FG doubly curved shallow shell in thermal environment using multiple scales method", *Compos. Struct.*, **256**, 113090. <https://doi.org/10.1016/j.compstruct.2020.113090>.
- Al Mukahal, F.H.H. and Sobhy, M. (2021), "Wave propagation and free vibration of FG graphene platelets sandwich curved beam with auxetic core resting on viscoelastic foundation via DQM", *Arch. Civ. Mech. Eng.*, **22**(1), 12. <https://doi.org/10.1007/s43452-021-00322-3>.
- Alazwari, M.A., Daikh, A.A. and Eltaher, M.A. (2022), "Novel quasi 3D theory for mechanical responses of FG-CNTs reinforced composite nanoplates", *Adv. Nano Res.*, **12**(2), 117-137. <https://doi.org/10.12989/anr.2022.12.2.117>.
- Allahkarami, F. and Tohidi, H. (2022), "Axisymmetric Postbuckling of Functionally Graded Graphene Platelets Reinforced Composite Annular Plate on Nonlinear Elastic Medium in Thermal Environment", *Int. J. Struct. Stab. Dy.*, **23**(5), 2350034. <https://doi.org/10.1142/S0219455423500347>.
- Alnujaie, A., Akba, E. D., Eltaher, M., and Assie, A. (2021), "Forced vibration of a functionally graded porous beam resting on viscoelastic foundation", *Geomech. Eng.*, **24**(1), 91-103. <http://doi.org/10.12989/gae.2021.24.1.091>
- Aris, H. and Ahmadi, H. (2022), "Combination resonance analysis of imperfect functionally graded conical shell resting on nonlinear viscoelastic foundation in thermal environment under multi-excitation", *J. Vib. Control.*, **28**(15-16), 2121-2144. <https://doi.org/10.1177/10775463211006527>.
- Assie, A.E., Mohamed, S.A., Shanab, R.A., Abo-bakr, R.M. and Eltaher, M.A. (2023), "Static buckling of 2D FG porous plates resting on elastic foundation based on unified shear theories", *J. Appl. Comput. Mech.*, **9**(1), 239-258. <https://doi.org/10.22055/jacm.2022.41265.3723>.
- Babaei, M., Kiarasi, F., Hossaeini Marashi, S.M., Ebadati, M., Masoumi, F. and Asemi, K. (2021), "Stress wave propagation and natural frequency analysis of functionally graded graphene platelet-reinforced porous joined conical-cylindrical-conical shell", *Wave Random Complex.*, <https://doi.org/10.1080/17455030.2021.2003478>.
- Basha, M., Daikh, A.A., Melaibari, A., Wagih, A., Othman, R., Almitani, K.H., Hamed, M.A., Abdelrahman, A. and Eltaher, M.A. (2022), "Nonlocal strain gradient theory for buckling and bending of FG-GRNC laminated sandwich plates", *Steel. Compos. Struct.*, **43**(5), 639-660. <https://doi.org/10.12989/scs.2022.43.5.639>.
- Chen, X., Zhao, J.L., She, G.L., Jing, Y., Luo, J. and Pu, H.Y. (2022a), "On wave propagation of functionally graded CNT strengthened fluid-conveying pipe in thermal environment", *Eur. Phys. J. Plus.*, **137**(10), 1158. <https://doi.org/10.1140/epjp/s13360-022-03234-0>.
- Chen, X., Zhao, J.L., She, G.L., Jing, Y., Pu, H.Y. and Luo, J. (2022b), "Nonlinear free vibration analysis of functionally graded carbon nanotube reinforced fluid-conveying pipe in thermal environment", *Steel. Compos. Struct.*, **45**(5), 641-652. <https://doi.org/10.12989/scs.2022.45.5.641>.
- Daikh, A.A., Belarbi, M.O., Salami, S.J., Ladmek, M., Belkacem, A., Houari, M.S.A., Ahmed, H.M. and Eltaher, M.A. (2023), "A three-unknown refined shear beam model for the bending of randomly oriented FG-CNT/fiber-reinforced composite laminated beams rested on a new variable elastic foundation", *Acta Mechanica*, 1-16. <https://doi.org/10.1007/s00707-023-03657-5>
- Daikh, A.A., Houari, M.S.A., Karami, B., Eltaher, M.A., Dimitri, R. and Tornabene, F. (2021), "Buckling analysis of CNTRC curved sandwich nanobeams in thermal environment", *Appl. Sci.*, **11**(7), 3250. <https://doi.org/10.3390/app11073250>.
- Ding, H.X. and She, G.L. (2021), "A higher-order beam model for the snap-buckling analysis of FG pipes conveying fluid", *Struct. Eng. Mech.*, **80**(1), 63-72. <https://doi.org/10.12989/sem.2021.80.1.063>.
- Ding, H.X. and She, G.L. (2023a), "Nonlinear resonance of axially moving graphene platelet-reinforced metal foam cylindrical shells with geometric imperfection", *Archiv. Civil Mech. Eng.*, **23**, 97. <https://doi.org/10.1007/s43452-023-00634-6>.
- Ding, H.X. and She, G.L. (2023b), "Nonlinear primary resonance behavior of graphene platelets reinforced metal foams conical shells under axial motion", *Nonlinear Dynam.*, **111**(15), 13723-13752. <https://doi.org/10.1007/s11071-023-08564-x>.
- Ding, H.X. and She, G.L. (2023c), "Nonlinear combined resonances of axially moving graphene platelets reinforced metal foams cylindrical shells under forced vibrations", *Nonlinear Dynam.*, <https://doi.org/10.1007/s11071-023-09059-5>.
- Ding, H.X., She, G.L. and Zhang, Y.W. (2022a), "Nonlinear buckling and resonances of functionally graded fluid-conveying pipes with initial geometric imperfection", *Eur. Phys. J. Plus.*, **137**, 1329. <https://doi.org/10.1140/epjp/s13360-022-03570-1>.
- Ding, H.X., Zhang, Y.W. and She, G.L. (2022b), "On the resonance problems in FG-GPLRC beams with different boundary conditions resting on elastic foundations", *Comput. Concrete*, **30**(6), 433-443. <https://doi.org/10.12989/cac.2022.30.6.433>.
- Ding, H.X., Eltaher, M.A. and She, G.L. (2023a), "Nonlinear low-velocity impact of graphene platelets reinforced metal foams cylindrical shell: Effect of spinning motion and initial geometric imperfections", *Aerosp. Sci. Tech.*, **140**, 108435.

- <https://doi.org/10.1016/j.ast.2023.108435>
- Ding, H.X., Zhang, Y.W. and She, G.L. (2023b), "Propagation characteristics of guided waves in CNTRCs plates resting on elastic foundations in a thermal environment", *Waves Random Complex Media*, <https://doi.org/10.1080/17455030.2023.2235611>.
- Ding, H.X., Liu, H.B., She, G.L. and Wu, F. (2023c), "Wave propagation of FG-CNTRC plates in thermal environment using the high-order shear deformation plate theory", *Comput. Concrete*, **32**(2), 207-215. <https://doi.org/10.12989/cac.2023.32.2.207>.
- Ding, H.X., Zhang, Y.W., Li, Y.P. and She, G.L. (2023d), "Nonlinear low-velocity impact response of graphene platelets reinforced metal foams doubly curved shells", *Steel Compos. Struct.*, **49**(3), 281-291. <https://doi.org/10.12989/scs.2023.49.3.281>.
- Ebrahimi, F. and Dabbagh, A. (2020), "Viscoelastic wave propagation analysis of axially motivated double-layered graphene sheets via nonlocal strain gradient theory", *Wave Random Complex*, **30**(1), 157-176. <https://doi.org/10.1080/17455030.2018.1490505>.
- Ebrahimi, F. and Seyfi, A. (2022), "On wave propagation characteristics of hygrothermally excited graphene foam plates", *Wave Random Complex*, <https://doi.org/10.1080/17455030.2022.2105416>.
- Ebrahimi, F., Mohammadi, K. and Barouti, M.M. (2021), "Wave propagation analysis of a spinning porous graphene nanoplatelet-reinforced nanoshell", *Wave Random Complex*, **31**(6), 1655-1681. <https://doi.org/10.1080/17455030.2019.1694729>.
- Gan, L.L. and She, G.L. (2023), "Nonlinear snap-buckling and resonance of FG-GPLRC curved beams with different boundary conditions", *Geomech. Eng.*, **32**(5), 541-551. <https://doi.org/10.12989/gae.2023.32.5.541>.
- Gan, L.L. and She, G.L. (2024), "Nonlinear low-velocity impact of magneto-electro-elastic plates with initial geometric imperfection", *Acta Astronautica*, **214**, 11-29. <https://doi.org/10.1016/j.actaastro.2023.10.016>.
- Gan, L.L., Xu, J.Q. and She, G.L. (2023), "Wave propagation of graphene platelets reinforced metal foams circular plates", *Struct. Eng. Mech.*, **85**(5), 645-654. <https://doi.org/10.12989/sem.2023.85.5.645>.
- Hashemi-Nejad, H., Saidi, A.R. and Bahaadini, R. (2022), "Wave propagation in rotating thin-walled porous blades reinforced with graphene platelets", *Zamm-Z Angew. Math. Me.*, **102**(9), e202100502. <https://doi.org/10.1002/zamm.202100502>.
- Hendi, A., Eltaher, M.A., Mohamed, S.A. and Attia, M. (2022), "Nonlinear thermal vibration of pre/post-buckled two-dimensional FGM tapered microbeams based on a higher order shear deformation theory", *Steel Compos. Struct.*, **41**(6), 787-802. <http://doi.org/10.12989/scs.2021.41.6.787>.
- Li, C. and Han, Q. (2021), "Analyzing wave propagation in graphene-reinforced nanocomposite annular plates by the semi-analytical formulation", *Mech. Adv. Mater. Struct.*, **28**(23), 2385-2398. <https://doi.org/10.1080/15376494.2020.1736698>.
- Li, C. and Han, Q. (2021), "Guided waves propagation in sandwich cylindrical structures with functionally graded graphene-epoxy core and piezoelectric surface layers", *J. Sandw. Struct. Mater.*, **23**(8), 3878-3901. <https://doi.org/10.1177/1099636220959034>.
- Li, C., Han, Q., Wang, Z. and Wu, X. (2020), "Analysis of wave propagation in functionally graded piezoelectric composite plates reinforced with graphene platelets", *Appl. Math. Model.*, **81**, 487-505. <https://doi.org/10.1016/j.apm.2020.01.016>.
- Li, Y.P., She, G.L., Gan, L.L. and Liu, H.B. (2023), "Nonlinear thermal post-buckling analysis of graphene platelets reinforced metal foams plates with initial geometrical imperfection", *Steel Compos. Struct.*, **46**(5), 649-658. <https://doi.org/10.12989/scs.2023.46.5.649>.
- Mahani, R.B., Eyvazian, A., Musharavati, F., Sebaey, T.A. and Talebizadehsardari, P. (2020), "Thermal buckling of laminated Nano-Composite conical shell reinforced with graphene platelets", *Thin. Wall. Struct.*, **155**, 106913. <https://doi.org/10.1016/j.tws.2020.106913>.
- Malikan, M., Wiczenbach, T. and Eremeyev, V.A. (2022), "Thermal buckling of functionally graded piezomagnetic micro- and nanobeams presenting the flexomagnetic effect", *Continuum Mech. Thermodynam.*, **34**(4), 1051-1066. <https://doi.org/10.1007/s00161-021-01038-8>.
- Martins, A.D., Goncalves, R. and Camotim, D. (2021), "Post-buckling behaviour of thin-walled regular polygonal tubes subjected to bending", *Thin. Wall. Struct.*, **166**, 108106. <https://doi.org/10.1016/j.tws.2021.108106>.
- Melaibari, A., Mohamed, S.A., Assie, A.E., Shanab, R.A. and Eltaher, M.A. (2023), "Static response of 2D FG porous plates resting on elastic foundation using midplane and neutral surfaces with Movable constraints", *Mathematics*, **10**(24), 4784. <https://doi.org/10.3390/math10244784>.
- Mohamed, S.A., Assie, A.E. and Eltaher, M.A. (2023), "Novel incremental procedure in solving nonlinear static response of 2D-FG porous plates", *Thin Wall. Struct.*, **189**, 110779. <https://doi.org/10.1016/j.tws.2023.110779>.
- Nguyen, T.P., Vu, M.D., Cao, V.D. and Vu, H.N. (2021), "Nonlinear torsional buckling of functionally graded graphene-reinforced composite (FG-GRC) laminated cylindrical shells stiffened by FG-GRC laminated stiffeners in thermal environment", *Polym. Compos.*, **42**(6), 3051-3063. <https://doi.org/10.1002/pc.26038>.
- Phuong, N.T., Dong, D.T., Van Doan, C. and Nam, V.H. (2022), "Nonlinear buckling of higher-order shear deformable stiffened FG-GRC laminated plates with nonlinear elastic foundation subjected to combined loads", *Aerosp. Sci. Technol.*, **127**, 107736. <https://doi.org/10.1016/j.ast.2022.107736>.
- Phuong, N.T., Nam, V.H., Trung, N.T., Duc, V.M., Loi, N.V., Thinh, N.D. and Tu, P.T. (2021), "Thermomechanical postbuckling of functionally graded graphene-reinforced composite laminated toroidal shell segments surrounded by Pasternak's elastic foundation", *J. Thermoplast. Compos.*, **34**(10), 1380-1407. <https://doi.org/10.1177/0892705719870593>.
- Ramezani, M., Rezaiee-Pajand, M. and Tornabene, F. (2022), "Nonlinear thermomechanical analysis of GPLRC cylindrical shells using HSDT enriched by quasi-3D ANS cover functions", *Thin. Wall. Struct.*, **179**, 109582. <https://doi.org/10.1016/j.tws.2022.109582>.
- Saiah, B., Bachene, M., Guemana, M., Chiker, Y. and Attaf, B. (2022), "On the free vibration behavior of nanocomposite laminated plates contained piece-wise functionally graded graphene-reinforced composite plies", *Eng. Struct.*, **253**, 113784. <https://doi.org/10.1016/j.engstruct.2021.113784>.
- Salehi, M., Gholami, R. and Ansari, R. (2022), "Nonlinear resonance of functionally graded porous circular cylindrical shells reinforced by graphene platelet with initial imperfections using higher-order shear deformation theory", *Int. J. Struct. Stab. Dy.*, **22**(6), 2250075. <https://doi.org/10.1142/S0219455422500754>.
- Shahgholian-Ghahfarokhi, D., Rahimi, G., Khodadadi, A., Salehipour, H. and Afrand, M. (2021), "Buckling analyses of FG porous nanocomposite cylindrical shells with graphene platelet reinforcement subjected to uniform external lateral pressure", *Mech. Based. Des. Struc.*, **49**(7), 1059-1079. <https://doi.org/10.1080/15397734.2019.1704777>.
- Shan, W.B. and She, G.L. (2023), "Nonlinear resonance of porous functionally graded nanoshells with geometrical imperfection", *Struct. Eng. Mech.*, **88**(4), 355-368.

- <https://doi.org/10.12989/sem.2023.88.4.355>.
- She, G.L. (2021), "Guided wave propagation of porous functionally graded plates: The effect of thermal loadings", *J. Therm. Stresses*, **44**(10)1289-1305. <https://doi.org/10.1080/01495739.2021.1974323>.
- She, G.L. and Ding, H.X. (2023), "Nonlinear primary resonance analysis of initially stressed graphene platelet reinforced metal foams doubly curved shells with geometric imperfection", *Acta Mech. Sin.*, **39**, 522392. <https://doi.org/10.1007/s10409-022-22392-x>.
- She, G.L. and Li, Y.P. (2022), "Wave propagation in an FG circular plate in thermal environment", *Geomech. Eng.*, **31**(6), 615-622. <https://doi.org/10.12989/gae.2022.31.6.615>.
- She, G.L., Ding, H.X. and Zhang, Y.W. (2022), "Wave propagation in a FG circular plate via the physical neutral surface concept", *Struct. Eng. Mech.*, **82**(2), 225-232. <https://doi.org/10.12989/sem.2022.82.2.225>.
- She, G.L., Liu, H.B. and Karami, B. (2021), "Resonance analysis of composite curved microbeams reinforced with graphene nanoplatelets", *Thin Wall. Struct.*, **160**, 107407. <https://doi.org/10.1016/j.tws.2020.107407>.
- Sun, D. and Luo, S.N. (2012), "Wave propagation and transient response of a functionally graded material plate under a point impact load in thermal environments", *Appl. Math. Model.*, **36**(1), 444-462. <https://doi.org/10.1016/j.apm.2011.07.023>.
- Trang, L.T.N. and Tung, H.V. (2022), "Thermally induced post-buckling of thin CNT-reinforced composite plates under nonuniform in-plane temperature distributions", *J. Thermoplast. Compos.*, **35**(12), 2331-2353. <https://doi.org/10.1177/0892705720962172>.
- Van Doan, C., Hung, V.T., Phuong, N.T. and Nam, V.H. (2022), "Torsional buckling and postbuckling behavior of stiffened FG-GRCL toroidal shell segments surrounded by elastic foundation", *Int. J. Comput. Mat. Sci.*, 2350001. <https://doi.org/10.1142/S204768412350001X>.
- Wang, Y. and Zhang, W. (2022), "On the thermal buckling and post-buckling responses of temperature-dependent graphene platelets reinforced porous nanocomposite beams", *Compos. Struct.*, **296**, 115880. <https://doi.org/10.1016/j.compstruct.2022.115880>.
- Wu, F. and She, G.L. (2023), "Wave propagation in double nanobeams in thermal environments using the Reddy's high-order shear deformation theory", *Adv. Nano Res.*, **14**(6), 495-506. <https://doi.org/10.12989/anr.2023.14.6.495>.
- Xiang, J., Lai, Y.L., Moradi, Z. and Khorami, M. (2023), "Wave propagation phenomenon of functionally graded graphene oxide powder-strengthened nanocomposite curved beam", *Solid State Commun.*, **369**, 115193. <https://doi.org/10.1016/j.ssc.2023.115193>.
- Xu, J.Q. and She, G.L. (2022), "Thermal post-buckling analysis of porous functionally graded pipes with initial geometric imperfection", *Geomech. Eng.*, **31**(3), 329-337. <https://doi.org/10.12989/gae.2022.31.3.329>.
- Xu, J.Q. and She, G.L. (2023a), "Thermal post-buckling of graphene platelet reinforced metal foams doubly curved shells with geometric imperfection", *Struct. Eng. Mech.*, **87**(1), 85-94. <https://doi.org/10.12989/sem.2023.87.1.085>.
- Xu, J.Q. and She, G.L. (2023b), "The effects of temperature and porosity on resonance behavior of graphene platelet reinforced metal foams doubly-curved shells with geometric imperfection", *Geomech. Eng.*, **35**(1), 81-93. <https://doi.org/10.12989/gae.2023.35.1.081>.
- Xu, J.Q. and She, G.L. (2023c), "Resonance behavior of functionally graded carbon nanotube-reinforced composites shells with spinning motion and axial motion", *Steel Compos. Struct.*, **49**(3), 325-335. <https://doi.org/10.12989/scs.2023.49.3.325>.
- Xu, J.Q. and She, G.L. (2024), "Thermal post-buckling and primary resonance of porous functionally graded beams: Effect of elastic foundations and geometric imperfection", *Comput. Concrete*, **32**(6), 543-551. <https://doi.org/10.12989/cac.2023.32.6.543>.
- Xu, J.Q., She, G.L., Li, Y.P. and Gan, L.L. (2023), "Nonlinear resonances of nonlocal strain gradient nanoplates made of functionally graded materials considering geometric imperfection", *Steel Compos. Struct.*, **47**(6), 795-811. <https://doi.org/10.12989/scs.2023.47.6.795>.
- Zenkour, A.M. and Sobhy, M. (2022), "Axial magnetic field effect on wave propagation in bi-layer FG graphene platelet-reinforced nanobeams", *Eng. Comput.*, **38**(2), 1313-1329. <https://doi.org/10.1007/s00366-020-01224-3>.
- Zhang, Y.W. and She, G.L. (2022), "Wave propagation and vibration of FG pipes conveying hot fluid", *Steel. Compos. Struct.*, **42**(3), 397-405. <https://doi.org/10.12989/scs.2022.42.3.397>.
- Zhang, Y.W. and She, G.L. (2023a), "Nonlinear low-velocity impact response of graphene platelet-reinforced metal foam cylindrical shells under axial motion with geometrical imperfection", *Nonlinear Dynamics*, **111**(7), 6317-6334. <https://doi.org/10.1007/s11071-022-08186-9>.
- Zhang, Y.W. and She, G.L. (2023b), "Nonlinear primary resonance of axially moving functionally graded cylindrical shells in thermal environment", *Mech. Adv. Mater. Struct.*, <https://doi.org/10.1080/15376494.2023.2180556>.
- Zhang, Y.W., Ding, H.X. and She, G.L. (2022), "Snap-buckling and resonance of functionally graded graphene reinforced composites curved beams resting on elastic foundations in thermal environment", *J. Therm. Stresses*, **45**(12), 1029-1042. <https://doi.org/10.1080/01495739.2022.2125137>.
- Zhang, Y.W., Ding, H.X. and She, G.L. (2023a), "Wave propagation in spherical and cylindrical panels reinforced with carbon nanotubes", *Steel Compos. Struct.*, **46**(1), 133-141. <https://doi.org/10.12989/scs.2023.46.1.133>.
- Zhang, Y.W., She, G.L. and Ding, H.X. (2023b), "Nonlinear resonance of graphene platelets reinforced metal foams plates under axial motion with geometric imperfections", *Eur. J. Mech. A-Solid.*, **98**, 104887. <https://doi.org/10.1016/j.euromechsol.2022.104887>.
- Zhang, Y.W., She, G.L., Gan, L.L. and Li, Y.P. (2023c), "Thermal post-buckling behavior of GPLRMF cylindrical shells with initial geometrical imperfection", *Geomech. Eng.*, **32**(6), 615-625. <https://doi.org/10.12989/gae.2023.32.6.615>.
- Zhang, Y.W., Ding, H.X., She, G.L. and Tounsi, A. (2023d), "Wave propagation of CNTRC beams resting on elastic foundation based on various higher-order beam theories", *Geomech. Eng.*, **33**(4), 381-391. <https://doi.org/10.12989/gae.2023.33.4.381>.
- Zhang, Y.W., She, G.L. and Eltahir, M.A. (2023e), "Nonlinear transient response of graphene platelets reinforced metal foams annular plate considering rotating motion and initial geometric imperfection", *Aerosp. Sci. Technol.*, **142**, 108693. <https://doi.org/10.1016/j.ast.2023.108693>.
- Zhang, Y.W. and She, G.L. (2024), "Combined resonance of graphene platelets reinforced metal foams cylindrical shells with spinning motion under nonlinear forced vibration", *Eng. Struct.*, **300**, 117177. <https://doi.org/10.1016/j.engstruct.2023.117177>.
- Zhang, Y.Y., Wang, X.Y., Zhang, X., Shen, H.M. and She, G.L. (2021), "On snap-buckling of FG-CNTRC curved nanobeams considering surface effects", *Steel Compos. Struct.*, **38**(3), 293-304. <https://doi.org/10.12989/scs.2021.38.3.293>.
- Zhao, J.L., Chen, X., She, G.L., Jing, Y., Bai, R.Q., Yi, J., Pu, H.Y. and Luo, J. (2022a), "Vibration characteristics of functionally graded carbon nanotube-reinforced composite double-beams in thermal environments", *Steel Compos. Struct.*, **43**(6), 797-808. <https://doi.org/10.12989/scs.2022.43.6.797>.

Zhao, J.L., She, G.L., Wu, F., Yuan, S.J., Bai, R.Q., Pu, H.Y., Wang, S.L. and Luo, J. (2022b), “Guided waves of porous FG nanoplates with four edges clamped”, *Adv. Nano. Res.*, **13**(5), 465-474. <https://doi.org/10.12989/anr.2022.13.5.465>.

CC